FIG. 13. Completion of Slope Shown in Fig. 12, with Erosion Control Fabric on Slope Face

- Slope face erosion protection

  Layers of reinforcement are commonly used so that the slope inclination can be increased. This will frequently result in surface erosion problems, especially when granular (free-draining) soil is used as the fill surrounding the Geogrid. In this case, it is important to provide slope face erosion protection. Fig. 13 shows a photograph of the completed Geogrid reinforced slope that has been faced with an erosion protection fabric. Deep-rooting shrubs were then planted on the slope face by cutting small holes in the erosion protection fabric.

In summary, important design factors for the construction of reinforced slopes include the construction of a key, mitigation of positive pore-water pressures in the reinforced slope by using granular (permeable) fill and installing a key drain and chimney drains, tipping the reinforcement into the slope to make it more effective, and installing an erosion control fabric and deep-rooting shrubs to reduce the potential for erosion of the slope face.

Discussion by P. de Buhan[5] and J. Salençon,[6] Member, ASCE

In this contribution by Professor Michalowski, a continuation of several papers, notably Michalowski and Zhao (1995), attention is paid to the stability analysis of reinforced slopes through a kinematic approach with special emphasis on the way the pullout failure mechanism of the reinforcement can be taken into account in the analysis. The discussers would like to add a few comments about the theoretical background of this paper and possible extensions.

As regards the distinction made by the author between the "continuum" and "structural" approaches, special interest should be given to the "mixed modeling" approach where the soil is modeled as a 3D continuum, the reinforcements being treated as 1D structural elements (beams) (Anthoine 1989). This approach, which does not refer to any homogenization procedure, may be applied to any kind of reinforcement pattern, whatever the distribution of the inclusions throughout the soil mass.

As an example, a computer program has been developed (de Buhan et al. 1993a,c), based upon this approach, for the stability analysis of reinforced soil structures, which makes use of rotational failure mechanisms within the framework of the yield design upper-bound method. It is suitable for any kind of reinforcement (nailing, tie-backs, geotextiles, etc.), multilayered soils, and various loading conditions including seismic effects. Shear and bending resistances of the reinforcements may also be taken into account in the design procedure, although their favorable effects on the stability of the structures turns out to be negligible in most cases (de Buhan and Salençon 1993). It is fully compatible with the Ultimate Limit State Design (ULSD) concept, illustrating the fact that the theory of yield design is the theoretical background of ULSD (de Buhan et al. 1993b).

A comparison has been made between the results of this program when a periodic distribution of homogeneous reinforcing elements in a homogeneous soil is assumed, and those given by the homogenization procedure. The comparison is actually meaningful since both approaches rely on the same class of failure mechanisms. It proves that the two points of view become equivalent under the foregoing assumptions provided that the spacing of the reinforcing inclusions be small enough in comparison with a typical length for the considered structure: e.g., for a vertical embankment with evenly distributed horizontal nails the obtained results are practically similar when the number of nails reaches 10 (de Buhan et al. 1989).

APPENDIX. REFERENCES

Anthoine, A. (1989). "Mixed modelling of reinforced soils within the framework of the yield design theory." *Comp. and Geotechnics*, 7, 67–82.

de Buhan, P., and Salençon, J. (1993). "A comprehensive stability analysis of soil nailed structures." *Eur. J. Mech., A/Solids*, Montrouge, France, 12(3), 325–345.

de Buhan, P., Dormieux, L., and Salençon, J. (1993a). "An interactive computer software for the yield design of reinforced soil structures." *Proc., Int. Conf. Comp. and Geotechnics*, Presses de l'ENPC, Paris, 181–188.

de Buhan, P., Dormieux, L., and Salençon, J. (1993b). "A theoretical approach to the Ultimate Limit State Design." *Proc., Conf. Limit State Design in Geotech. Engrg., DGI Bull. No. 10*, Vol. 2, Copenhagen, 429–438.

de Buhan, P., Dormieux, L., and Salençon, J. (1993c). "Stability analysis of reinforced soil retaining structures using the yield design theory." *Proc., Int. Conf. Retaining Struct.*, Thomas Telford, London, 618–627.

Discussion by Patrick Lemonnier[7]

The author has investigated the stability of the reinforced slopes by using the upper-bound method of the limit analysis theory. The discusser wishes to comment on the assumption made by the author concerning the determination of the required strength of the reinforcement. For this determination, a rotational log-spiral collapse mechanism is used. As is well known, this mechanism moves as a rigid body and the internal energy dissipation takes place only along the log-spiral surface.

In the opinion of the discusser, this assumption is valid in the case of inextensible reinforcements, but not in the case of extensible reinforcements. In the latter case, the mobilization of the tensions induces relatively important deformation of the reinforcement sheets (Gourc et al. 1988; Lemonnier 1995). Though the author has not explicitly dealt with any special reinforcement types, the results of his new method are compared to those obtained from methods that are only valid for

[5]Prof., Ecole Nationale des Ponts et Chaussées, CERMMO, 6 et 8 avenue Blaise Pascal, 77455 Marne-la-Vallee Cedex 2, France. E-mail: debuhan@enpc.fr

[6]Prof., Ecole Polytechnique, Dept. of Mech., 91128 Palaiseau Cedex, France. E-mail: dieu@poly.polytechnique.fr

[7]Postdoctoral Res., Aalborg Univ., Dept. of Civ. Engrg., Sohngaardsholmsvej 57, DK-9000 Aalborg, Denmark.

geogrids (Schmertmann et al. 1987), or more generally for the full range of polymer reinforcement materials (Jewell 1990). Thus, the discusser would very much appreciate the clarification of the author concerning the assumption of a rigid body movement of the soil mass, with no energy dissipation within this mass, and considering this type of reinforcement.

APPENDIX. REFERENCES

Gourc, J. P., Ratel, A., and Gotteland, P. (1988). "Design of reinforced soil retaining walls: Analysis and comparison of existing methods and proposal for a new approach." *The application of polymeric reinforcement in soil retaining structures, NATO Asi series—applied sciences*, Jarrett and McGown, eds., Vol. 147, 24–67.

Lemonnier, P. (1995). "Application de la méthode variationnelle au problème de la stabilité des talus renforcés par des nappes géosynthétiques," PhD thesis, INSA Lyon, France.

Closure by Radoslaw L. Michalowski[8]

The writer thanks Professors de Buhan and Salençon for their comments and interest in the paper. The method classified as the structural approach can indeed be considered also as "mixed modeling," since in the analysis the soil is taken as a continuum and the reinforcement as structural members. While it was convenient to represent the strength of reinforcement in terms of its average (or distributed) strength, k_t, the reinforcement sheets were considered as separate structural components in calculations of the length.

Both the structural and the continuum approach can be used in stability analysis of slopes. The gap in the calculated amount (or strength) of reinforcement necessary to maintain stability, using the two approaches, decreases with an increase in the number of layers, as the discussers noticed. There are some applications, however, where the homogenization technique cannot be used, for instance, in embankments reinforced with one or two geosynthetic layers. Also, the contribution of the reinforcement shear strength (and resistance to bending) requires that the structural approach be used, as presented by de Buhan and Salençon (1993). Calculations of the length of reinforcement sheets also require that they be considered as separate structural elements. In calculations of the length, the stress on reinforcement in the pullout force expression was taken as being approximately equal to the overburden weight. While such an assumption is reasonable (and generally accepted), the calculated length can no longer be proved a rigorous bound to a true solution; it is, however, a good estimate of the length. It did not come as a surprise that the calculated reinforcement length necessary to prevent failure was dependent on the number of layers.

Drs. Ausilio and Conte dispute the nature (or interpretation) of the term containing the influence of the pore-water pressure in the energy balance equation. The discussers apply the method used in the paper to a retaining wall problem, to indicate that it predicts a load inconsistent with the classical solution. The writer thanks the discussers for their interest in the paper and the effort they made to derive their equations, but he disagrees with their conclusions. In particular, (37) and (38) derived by Ausilio and Conte, which are the basis for their conclusions, are not consistent with the method proposed by the writer, and they predict incorrect results indeed.

To alleviate some of the questions with the interpretation of the method suggested in the paper, it is useful to investigate the work of the water pressure acting on a grain (or particle) during a small displacement increment of the grain. Consider first a pore-water pressure field with constant hydraulic head (zero hydraulic head gradient) [Fig. 14(a)]. Let the soil deform, for instance, due to applied load **P**, but the pore pressure field remain stationary. Consider particle A, which moves by displacement increment $\delta\mathbf{u}$. Pore-water pressure is an external load with respect to particle A, and its work on the particle displacement $\delta\mathbf{u}$ is exactly equal to the work of the buoyancy force acting on that particle. Notice that the net work of pore-water pressure on a horizontal displacement of a particle would be equal to zero. Now let particle B in Fig. 14(b) move by $\delta\mathbf{u}$. The work done by the pore-water pressure acting on the particle is now equal to the work of the buoyancy force (acting on particle B) plus the work of the seepage force. The work of both the buoyancy force and the seepage force must be included in analysis of stability of slopes.

In order to find a convenient way to include both forces in the kinematic approach of limit analysis, consider first the product of the pore-water pressure (u) and the rate of the volumetric strain ($\dot{\varepsilon}_{ii}$) of the soil $-u\dot{\varepsilon}_{ii}$. Such a product represents the rate of work of u on the volumetric expansion of the skeleton (pore-water pressure is assumed to be unaffected by the skeleton deformation as in a drained process). Because the dilatancy is considered a negative strain in soil mechanics convention, the minus sign is included to indicate that positive (compressive) pore pressure does positive work on skeleton expansion. This product is related to the work of the buoyancy force and the seepage force (Michalowski 1995); therefore, it is useful to investigate its integral over the volume of the entire failure mechanism. This investigation was not included in the original paper, but it is essential in order to give the physical interpretation to the term disputed by the discussers.

Let the vector of the displacement velocity in a failure mechanism be $\mathbf{v}_i$ [$\mathbf{v}_i$ is a function of x, y, z, or x_i ($i = 1, 2, 3$)]. Derivative $\partial/\partial x_i$ of the product $u\mathbf{v}_i$ is $\mathbf{v}_i\,\partial u/\partial x_i + u\,\partial \mathbf{v}_i/\partial x_i$, and since $\partial \mathbf{v}_i/\partial x_i = -\dot{\varepsilon}_{ii}$ (summation convention holds), one can write

$$-\int_V u\dot{\varepsilon}_{ii}\,dV = \int_V \frac{\partial}{\partial x_i}(u\mathbf{v}_i)\,dV - \int_V \frac{\partial u}{\partial x_i}\mathbf{v}_i\,dV$$

$$= \int_S u n_i \mathbf{v}_i\,dS - \int_V \frac{\partial u}{\partial x_i}\mathbf{v}_i\,dV \tag{40}$$

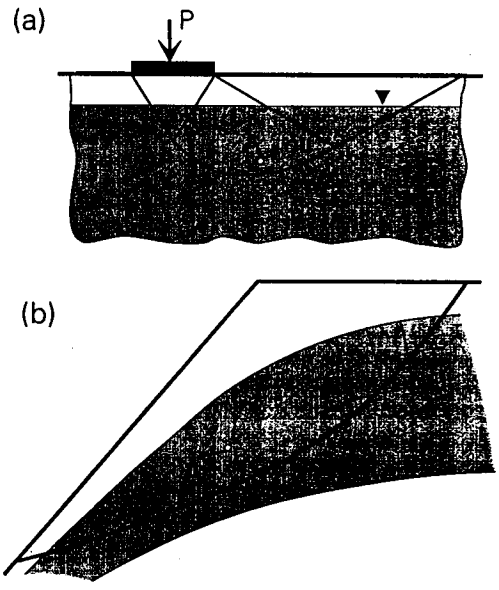

FIG. 14. Examples of Pore Water Pressure Distribution: (a) Stationary Water with Hydrostatic Distribution of Pore Pressure; (b) Schematic of Water Flow in Slope

[8]Assoc. Prof., Dept. of Civ. Engrg., The Johns Hopkins Univ., Baltimore, MD 21218.

where S = surface bounding volume V of the failure mechanism; and n_i = outward unit vector normal to surface S. The divergence theorem was used in (40) to transform the volume integral into the surface integral. The hydraulic head, h, (with the omission of the kinetic part) is $h = (u/\gamma_w) + Z$, where Z is the elevation head. Substitution of u from this expression into (40) yields

$$-\int_V u\dot{\varepsilon}_{ii}\,dV = \int_S un_i v_i\,dS - \gamma_w \int_V \frac{\partial h}{\partial x_i} v_i\,dV + \gamma_w \int_V \frac{\partial Z}{\partial x_i} v_i\,dV \tag{41}$$

Notice that the second term on the right-hand side of (41) represents the integral of the rate of work of the seepage force $(-\gamma_w\,\partial h/\partial x_i)$ over the entire mechanism, and the third term is the work rate of the buoyancy force in the entire volume of the failure mechanism. The first term on the right-hand side represents the work rate of the pore water pressure on boundary S. It was noticed earlier (Michalowski 1995) that for slopes with a phreatic surface contained within the soil, this term is equal to zero. Consequently, for such slopes, the work rate of the seepage and buoyancy forces is equal to the term on the left-hand side of (41), and this term was included in (1) of the original paper. Ausilio and Conte applied this term in calculations of the load on a retaining wall, arrived at (37), and noticed that (37) leads to incorrect values of load P_t on the wall. It does indeed, since in the retaining wall problem the first term on the right-hand side of (41) is no longer zero. The work rate of the seepage and buoyancy forces, $\dot{W}_u$, for the wall problem is

$$\dot{W}_u = -\int_V u\dot{\varepsilon}_{ii}\,dV - \int_S un_i v_i\,dS \tag{42}$$

and both terms in (42) need to be included in the analysis.

In the following paragraph the expression for the force acting on the wall is derived to show that the expression in (42) leads to correct results. For the retaining wall problem the expression in (34) needs to have an additional term due to the work rate of force P [Fig. 15(a)]

$$\dot{D} = \dot{W}_P + \dot{W}_\gamma + \dot{W}_u \tag{43}$$

This is an abbreviated form of (1) from the original paper. The hodograph for the problem is shown in Fig. 15(b). The wedge moves with velocity v, and the wall moves horizontally with velocity $v\sin(\Omega + \varphi)$. Thus, sliding on the wall surface occurs with sliding vector magnitude of $[v] = v\cos(\Omega + \varphi)$ (see hodograph), and the rate of work dissipation associated with this sliding is

$$\dot{D} = Pv \sin\delta \cos(\Omega + \varphi) \tag{44}$$

where δ is the wall friction angle. In the absence of cohesion the work dissipation rate along the failure surface is zero. The work rate of force P and the soil weight are

$$\dot{W}_P = -Pv\cos\delta \sin(\Omega + \varphi) \tag{45}$$

and

$$\dot{W}_\gamma = \frac{1}{2}\gamma H^2 v \tan\Omega \cos(\Omega + \varphi) \tag{46}$$

respectively. The specific forms of the terms in (42) now become

$$\dot{W}_u = \frac{1}{2}\gamma_w H^2 v \frac{\sin\varphi}{\cos\Omega} - \frac{1}{2}\gamma_w H^2 v \sin(\Omega + \varphi) \tag{47}$$

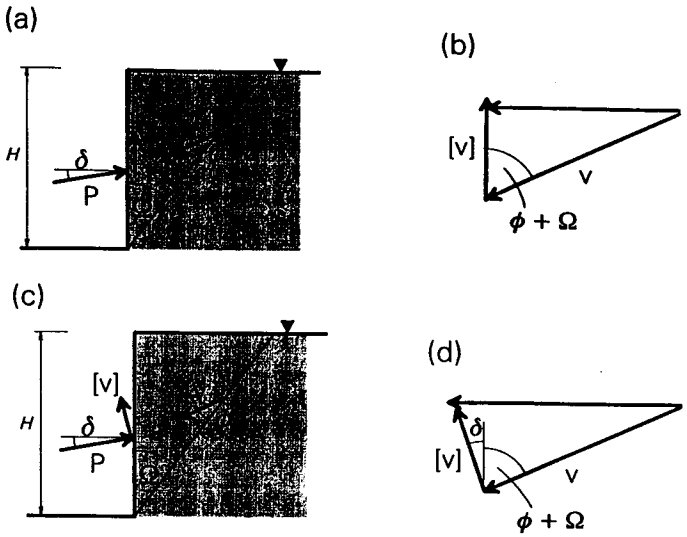

FIG. 15. Retaining Wall Load Problem: (a) Schematic for Analysis with Explicit Calculations of Work Dissipation on Wall Interface; (b) Hodograph; (c) Schematic for Alternative Method of Calculations; (d) Hodograph

The first term on the right-hand side of (42) now includes only the work of u along the failure surface, since dilation occurs only there. Upon substitution of (44)–(47) into (43), and rearranging, one obtains

$$P_n = \frac{1}{2}(\gamma - \gamma_w)H^2 \frac{\tan\Omega\cos(\Omega + \varphi)}{\sin(\Omega + \varphi) + \tan\delta\cos(\Omega + \varphi)} = \frac{1}{2}k_a(\gamma - \gamma_w)H^2 \tag{48}$$

where $P_n = P\cos\delta$. Notice that (48) is consistent with the classical solution, and it is identical to (35). The expression in (43) leads to the wall load caused by the soil, and the load due to hydrostatic pressure, $\gamma_w H^2/2$, can be added to (48) to obtain the total load as in (36). The discussers, however, obtained (37) instead of (48), because of the omission of the second term in (47), and interpreted it as a total load. The expression in (37) is not correct.

The rate of work dissipation was calculated here explicitly in (44). However, this is possible only when sliding on the interface occurs with a uniform velocity (otherwise the distribution of load needs to be known for calculations of work dissipation). To make calculations possible for cases where sliding is not uniform, one can assume that the sliding vector is inclined at the angle of wall friction to the interface. Such an assumption does not violate kinematical admissibility of the failure mechanism. Consequently, the sliding vector and the force acting on the wall are mutually orthogonal, and the dissipation rate becomes zero. Of course, this technique can also be applied to the simple example where the sliding velocity is uniform [Fig. 15(c and d)]. Such a method was suggested independently by Collins (1969) for compression of a metal block between two rigid dies, and by Mróz and Drescher (1969) for a hopper flow problem; it was also used by Chen (1975). The limit force on the retaining wall calculated in such a manner, with inclusion of the pore-water pressure influence as suggested here, is identical to that in (48). The discussers followed this method only for the case where $\delta = \varphi$, and arrived at (38), which is incorrect again, because of the omission of one term in the calculation of the influence of the pore-water pressure.

The discussers mention that their (37) "is not a rigorous upper bound." Even if it were correctly derived, it would not be an upper but a lower bound. The kinematic theorem of limit analysis yields an upper bound to active limit forces (forces

for which the work rate in the failure process is positive), and a lower bound to reactions. The force calculated here is the wall reaction, whose work rate during failure is negative [see (45)]. To find the best estimate of P, one needs to find Ω such that P is a maximum (best lower bound).

The charts were produced in the paper for slopes with uniform spacing of reinforcement; however, calculations for slopes with a triangular distribution of "smeared" strength were also carried out, and compared to those for $r_u > 0$ obtained by means of the limit equilibrium method (Jewell 1990). They appear to be identical.

In conclusion, the method suggested for inclusion of the buoyancy and seepage forces in the kinematic limit analysis is a rigorous approach leading to a strict bound on the true solution. All terms associated with this approach, which appear in the energy balance equation, have a clear physical interpretation.

Finally, the discussers suggest that the kinematic approach can be used to arrive at reinforcement for slopes subjected to seismic loads. Indeed, such calculations were recently performed for both the strength and the length of reinforcement, and for both uniform and nonuniform distribution (Michalowski, in press, 1998).

The writer also thanks Dr. Lemonnier for his interest in the paper, and the comment on the rigid rotation collapse mechanism used in the analysis. The discusser points out that mobilization of the tensile force in the reinforcement may be associated with an elastoplastic deformation process in the entire soil mass.

The kinematic approach of limit analysis belongs to the class of limit state techniques where the process prior to failure is not analyzed. The stiffness of reinforcement does not enter the analysis, and the question as to whether the results are applicable to extensible or inextensible reinforcement cannot be addressed explicitly. For the same reason the progression of failure and size effects are not considered. For that, a numerical approach needs to be used (such as the finite-element method) where both the soil and reinforcement are modeled as elastoplastic materials with a frictional (at the very least) soil-reinforcement interface. However, the results from limit state techniques have been used in the past for both inextensible reinforcement (such as metal strips) and extensible inclusions (such as synthetic sheets).

The method used in the paper is based on the energy rate balance equation written for an incipient failure process. The process of reinforcement force mobilization takes place prior to failure, and not just in the neighborhood of what later becomes the failure surface. Such a process is likely to be elastoplastic, in which some energy is dissipated and some is stored in the soil mass. However, at the instant of failure the process becomes perfectly plastic, without further increase in elastic energy, and the rigid rotation was found to be the most adverse collapse mode. The kinematic approach of limit analysis leads to the upper bound on the limit load on the slope, or the lower bound to the strength of reinforcement necessary to prevent failure. Any kinematically admissible mechanism provides the lower bound to the reinforcement strength. Out of the different mechanisms considered, the rigid rotation yields the maximum strength (the best lower bound), and therefore it was used to produce the charts.

The comments of Dr. Day are appreciated. However, the paper was on stability of reinforced slopes, and the objective was to present a rational stability analysis, concluded with charts that can be used to design the amount of reinforcement necessary to prevent collapse of slopes. Stability analysis is only a part of the entire design process, which must, of course, include such issues as secondary reinforcement, drainage, erosion protection, constructability, possible damage of geosynthetics prior to installation, etc.

Errata. The following corrections should be made to the original paper:

In Table 1, column 4 refer to Eq. (24) instead of Eq. (10).

In Eq. (27), the first minus sign should be replaced with a plus.

In Eq. (30), α should be replaced with θ_h.

APPENDIX. REFERENCES

Collins, I. F. (1969). "The upper-bound theorem for rigid/plastic solids generalized to include Coulomb friction." *J. Mech. Phys. Solids*, 17, 323–338.

Michalowski, R. L. (1998). "Soil reinforcement for seismic design of geotechnical structures." *Comp. and Geotechnics*, in press.

Mróz, Z., and Drescher, A. (1969). "Limit plasticity approach to some cases of flow of bulk solids." *J. Engrg. for Industry, Trans. ASME*, 51, 357–364.

MODIFIED NEWMARK MODEL FOR SEISMIC DISPLACEMENTS OF COMPLIANT SLOPES[a]

Discussion by Robert W. Day,[3] Fellow, ASCE

The authors present an interesting paper on the development of a modified Newmark analysis for estimation of the permanent displacement of slopes in earthquakes. The authors conclude that for the decoupled procedure, the permanent displacement is underpredicted for relatively thin and/or soft failure masses. The discusser believes that there may be other cases where the earthquake deformation is underpredicted, such as the two cases described here.

- Reduction of shear strength during earthquake

  The first case deals with the reduction of shear strength during the California Northridge earthquake (January 17, 1994; magnitude 6.7). The site is located about 11 km (7 mi) southwest of the epicenter (Day and Poland 1996). Using the EQSEARCH (Blake 1989) computer program, the estimated peak ground acceleration at the site was $0.55g$. The earthquake caused the reactivation of landslide debris (Fig. 15) which caused damage to the property as shown in Figs. 16–18. Subsurface exploration discovered the presence of old fractures in the landslide debris filled with gypsum as well as recent open fractures due to the earthquake. An interesting feature of this case was that the landslide debris continued to move after the earthquake as shown by the inclinometer readings (Fig. 19). The results of the earthquake investigation revealed that the earthquake opened up fractures in the landslide debris, which reduced the factor of safety, and reactivated the landslide movement.
- Earthquake-induced slope deformation of loose cohesionless soils

  The second case deals with slope movement due to earthquake-induced deformation of loose cohesionless

[a]July 1997, Vol. 123, No. 7, by Steven L. Kramer and Matthew W. Smith (Paper 12083).

[3]Chf. Engr., American Geotechnical, 5764 Pacific Ctr. Blvd., Ste. 112, San Diego, CA 92121.